

η -Scaling of $dN_{\text{ch}}/d\eta$ at $\sqrt{s_{NN}} = 200$ GeV by the PHOBOS Collaboration and the Ornstein-Uhlenbeck stochastic process

Minoru Biyajima^{1,2} and Takuya Mizoguchi³

¹*Department of Physics, Faculty of Science, Shinshu University, Matsumoto
390-8621, Japan*

²*Niels Bohr Institute, DK-2100, Copenhagen, Denmark*

³*Toba National College of Maritime Technology, Toba 517-8501, Japan*

(Received November 29, 2018)

Using the latest data concerning $dN_{\text{ch}}/d\eta$ at $\sqrt{s_{NN}} = 200$ GeV, we have analyzed them by means of stochastic theory named the Ornstein-Uhlenbeck process with two sources. Moreover, we display that $z_r = \eta/\sqrt{\langle\eta^2\rangle} = \eta/\eta_{\text{rms}}$ scaling with centrality cuts are described by two Gaussian distributions.

1. *Introduction* In previous papers,¹⁾ we have shown that there is an η -scaling in the charged multiplicity distributions $dN_{\text{ch}}/d\eta$ or $(N_{\text{ch}})^{-1}dN_{\text{ch}}/d\eta = dn/d\eta$ at $\sqrt{s_{NN}} = 130$ GeV by PHOBOS Collaboration.²⁾ Those distributions have been explained by a stochastic approach named the Ornstein-Uhlenbeck (OU) process with the evolution parameter t , the frictional coefficient γ and the variance σ^2 :

$$\frac{\partial P(y, t)}{\partial t} = \gamma \left[\frac{\partial}{\partial y} y + \frac{1}{2} \frac{\sigma^2}{\gamma} \frac{\partial^2}{\partial y^2} \right] P(y, t). \quad (1)$$

Introducing two sources at $\pm y_{\text{max}} = \ln(\sqrt{s_{NN}}/m_N)$ at $t = 0$ and $P(y, 0) = 0.5[\delta(y + y_{\text{max}}) + \delta(y - y_{\text{max}})]$, we obtain the following distribution function for $dn/d\eta$ (assuming $y \approx \eta$) using the probability density $P(y, t)$ ¹⁾

$$\frac{dn}{d\eta} = \frac{1}{\sqrt{8\pi V^2(t)}} \left\{ \exp \left[-\frac{(\eta + \eta_{\text{max}} e^{-\gamma t})^2}{2V^2(t)} \right] + \exp \left[-\frac{(\eta - \eta_{\text{max}} e^{-\gamma t})^2}{2V^2(t)} \right] \right\}, \quad (2)$$

where $V^2(t) = (\sigma^2/2\gamma)p$ with $p = 1 - e^{-2\gamma t}$.

On the other hand, in Ref. 3), PHOBOS Collaboration has reported new analyses at 200 GeV. Thus, we are interested in comparisons of our results in Ref. 1) with theoretical analyses of data in Ref. 3), in particular Eq. (2) and its $z_r = \eta/\eta_{\text{rms}}$ ($\eta_{\text{rms}} = \sqrt{\langle\eta^2\rangle}$) scaling function with $z_{\text{max}} = \eta_{\text{max}}/\eta_{\text{rms}}$ and $V_r^2(t) = V^2(t)/\eta_{\text{rms}}^2$.

$$\frac{dn}{dz_r} = \frac{1}{\sqrt{8\pi V_r^2(t)}} \left\{ \exp \left[-\frac{(z_r + z_{\text{max}} e^{-\gamma t})^2}{2V_r^2(t)} \right] + \exp \left[-\frac{(z_r - z_{\text{max}} e^{-\gamma t})^2}{2V_r^2(t)} \right] \right\}. \quad (3)$$

First we have to examine η scaling of $dn/d\eta$ in a semi-phenomenological point of view. After analyses in terms of Eqs. (2) and (3), we examine the meaning of the evolution parameter t with γ , assigning a physical dimension [second] to it. Finally concluding remarks are given.

2. *Semi-phenomenological analyses of data* In Fig. 1, we show distributions of $dn/d\eta$. As is seen in Fig. 1, the intercepts of $dn/d\eta|_{\eta=0}$ with different centrality cuts are located in the following narrow interval

$$\left. \frac{dn}{d\eta} \right|_{\eta=0} = c = 0.123 - 0.130. \quad (4)$$

We can observe that the η -scaling approximately holds at $\sqrt{s_{NN}} = 200$ GeV.

Next, we should examine a power-like law in $(0.5\langle N_{\text{part}} \rangle)^{-1} (dN_{\text{ch}}/d\eta)|_{\eta=0}$ ($\langle N_{\text{part}} \rangle$ being number of participants) which is proposed by WA98 Collaborations⁴⁾ as

$$\frac{1}{0.5\langle N_{\text{part}} \rangle} \left. \frac{dN_{\text{ch}}}{d\eta} \right|_{\eta=0} = A \langle N_{\text{part}} \rangle^\alpha. \quad (5)$$

As seen in Fig. 2, it can be stressed that the power-like law holds fairly well^{*)}. Using estimated parameters A and α , we can express c as

$$c = \frac{0.5\langle N_{\text{part}} \rangle}{N_{\text{ch}}} \times (2.05)\langle N_{\text{part}} \rangle^{0.101}. \quad (6)$$

They are shown in Table I. The intercepts show weak decreasing behavior as the centrality cut increases.

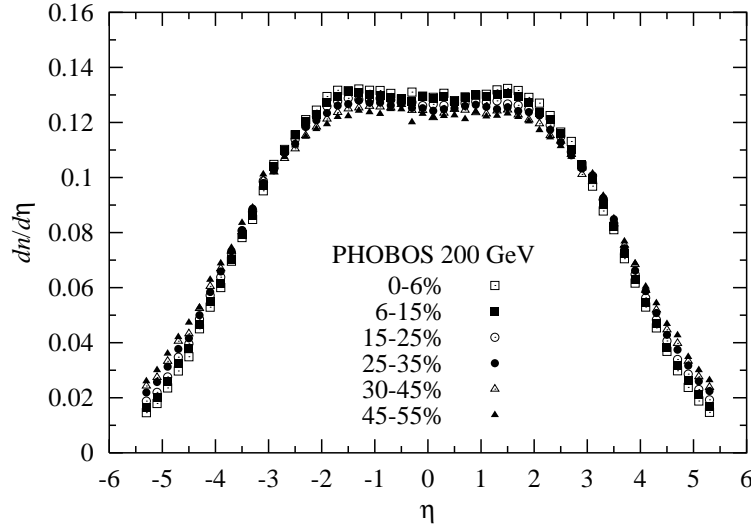


Fig. 1. $dn/d\eta$ with different centrality cuts.³⁾

3. Analyses of data by Eqs. (2) and (3)

3.1 *Explanation of $dn/d\eta$ by Eq. (2)* This time $\pm\eta_{\text{max}} = \pm 5.4$ are taken. The estimated parameters $V^2(t)$, p , $c(\text{Th}) = (1/\sqrt{2\pi V^2(t)}) \cdot \exp[-(\eta_{\text{max}} e^{-\gamma t})^2 / 2V^2(t)]$ and χ^2 are shown in Table II. The results are shown in Fig. 3. To describe the dip structures, the finite evolution time is necessary in our approach.

^{*)} According to Ref. 4), this law suggests the following picture: The incoming particles lose their memory and every participants contributes a similar amount of energy to particle production.

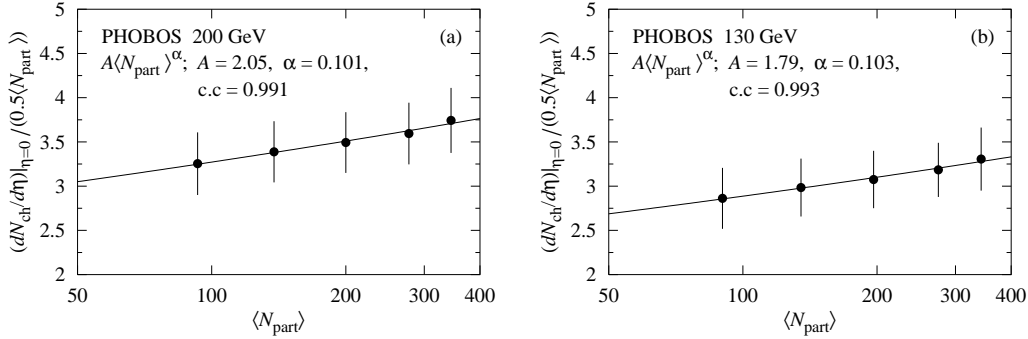


Fig. 2. Determination of the parameters A and α . The method of linear regression is used. The correlation coefficient (c.c.) is 0.991 (200 GeV). From data at 130 GeV we have $A = 1.79$, $\alpha = 0.103$ and c.c. = 0.993.

Table I. Empirical examination of Eq. (6) ($\sqrt{s_{NN}} = 200$ GeV).

centrality (%)	35–45	25–35	15–25	6–15	0–6
$\langle N_{\text{part}} \rangle$	93 ± 5	138 ± 6	200 ± 7.5	277 ± 8.5	344.5 ± 11
$N_{\text{ch}}^{(\text{Ex})}$	1230 ± 60	1870 ± 90	2750 ± 140	3860 ± 190	4960 ± 250
c (Ex)	0.123 ± 0.012	0.124 ± 0.012	0.127 ± 0.012	0.129 ± 0.012	0.130 ± 0.012
c (Eq. (6))	0.122 ± 0.009	0.124 ± 0.008	0.127 ± 0.008	0.130 ± 0.008	0.128 ± 0.008

Table II. Parameter values obtained in our analyses using Eq. (2). The evolution of $P(y, y_{\text{max}}, t)$ in Eq. (2), i.e., $dn/d\eta$ ($y \approx \eta$), is stopped at minimum values of χ^2 . Here, $\delta p = 0.004\text{--}0.006$ and $\delta c_t = 0.005\text{--}0.006$. (n.d.f. means the number of degree of freedom.) Values of η_{rms} are also shown. Notice that $c^*(\text{Th}) = c(\text{Th}) \cdot N_{\text{ch}}^{(\text{Th})}/N_{\text{ch}}^{(\text{Ex})}$. This ratio is needed for correction for $|\eta| > 5.4$.

centrality (%)	45–55	35–45	25–35	15–25	6–15	0–6
p	$0.855 \pm \delta p$	$0.861 \pm \delta p$	$0.864 \pm \delta p$	$0.868 \pm \delta p$	$0.873 \pm \delta p$	$0.876 \pm \delta p$
$V^2(t)$	3.62 ± 0.26	3.49 ± 0.23	3.31 ± 0.20	3.09 ± 0.17	2.95 ± 0.15	2.79 ± 0.13
$N_{\text{ch}}^{(\text{Th})}$	780 ± 13	1270 ± 21	1930 ± 30	2821 ± 43	3951 ± 60	5050 ± 77
$c^*(\text{Th})$	$0.121 \pm \delta c_t$	$0.123 \pm \delta c_t$	$0.124 \pm \delta c_t$	$0.125 \pm \delta c_t$	$0.127 \pm \delta c_t$	$0.127 \pm \delta c_t$
$\chi^2/\text{n.d.f.}$	1.07/51	0.91/51	0.88/51	1.18/51	1.06/51	1.46/51
$\eta_{\text{rms}} = \sqrt{\langle \eta^2 \rangle}$	2.57	2.54	2.51	2.48	2.45	2.42

3.2 Comparison with other approaches First we consider a problem between the role of Jacobian and dip structure at $\eta \approx 0$. The authors of Refs. 5) and 6) have explained $dN_{\text{ch}}/d\eta$ by means of the Jacobian between the rapidity variable (y) and the pseudorapidity (η): The following relation is well known

$$\frac{dn}{d\eta} = \frac{p}{E} \frac{dn}{dy} = \frac{\cosh \eta}{\sqrt{1 + m^2/p_t^2 + \sinh^2 \eta}} \frac{dn}{dy}, \quad (7)$$

where $dn/dy = (1/\sqrt{2\pi V^2(t)}) \exp[-y^2/2V^2(t)]$. It is worthwhile to examine whether or not $dn/d\eta$ at $\sqrt{s_{NN}} = 200$ GeV can be explained by Eq. (7). As is seen in Fig. 4, for $dn/d\eta$ in the full phase space ($|\eta| < 5.4$), it is difficult to explain the η distribution. On the other hand, if we restrict the central region ($|\eta| < 4$), i.e., neglecting the data in $4.0 < |\eta| < 5.4$, we have better description. These results are actually

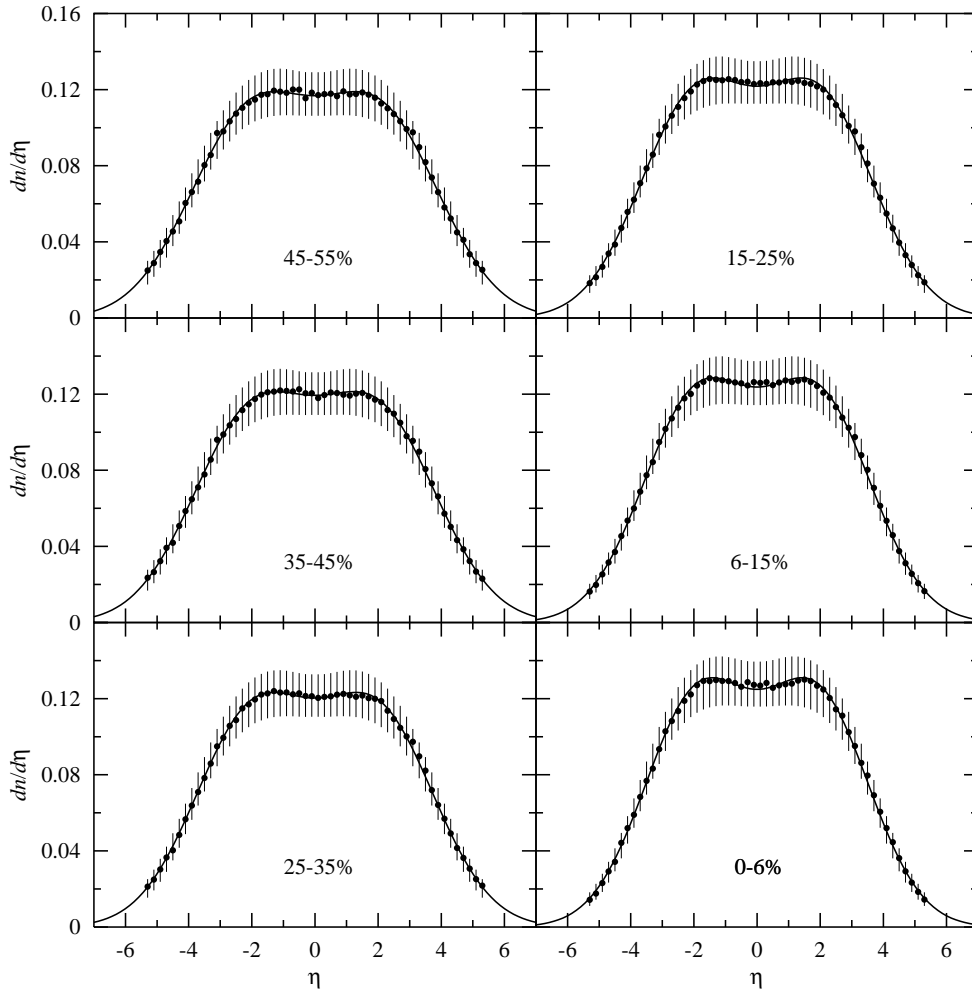


Fig. 3. Analyses of $dn/d\eta$ with centrality cuts using Eq. (2). (See Table II.)

utilized in Refs. 5) and 6). In other words, this fact suggests us that we have to consider other approaches to explain the dip structure in central region as well as the behavior in the fragmentation region. In our case it is the stochastic theory named the OU process with two sources at $\pm y_{\max}$ and at $t = 0$.

3.3 z_r scaling in $dn/d\eta$ distributions The values of $\eta_{\text{rms}} = \sqrt{\langle \eta^2 \rangle}$ are calculated in Table II. The $z_r = \eta/\eta_{\text{rms}}$ distributions are shown in Fig. 5(a). As seen there, z_r scaling in $dn/d\eta$ distributions with different centrality cuts holds at $\sqrt{s_{NN}} = 200$ GeV. To compare z_r scaling at 200 GeV with one at 130 GeV,¹⁾ we show the latter in Fig. 5(b). It is difficult to distinguish them. This coincidence means that there is no change in dn/dz_r as colliding energy increases, except for the region of $|z_r| \gtrsim 2.2$.

4. Interpretation of the evolution parameter t with γ In our present treatment the evolution parameter t and the frictional coefficient γ are dimensionless. When we assign the meaning of second [s] to t , the frictional coefficient γ has the dimension

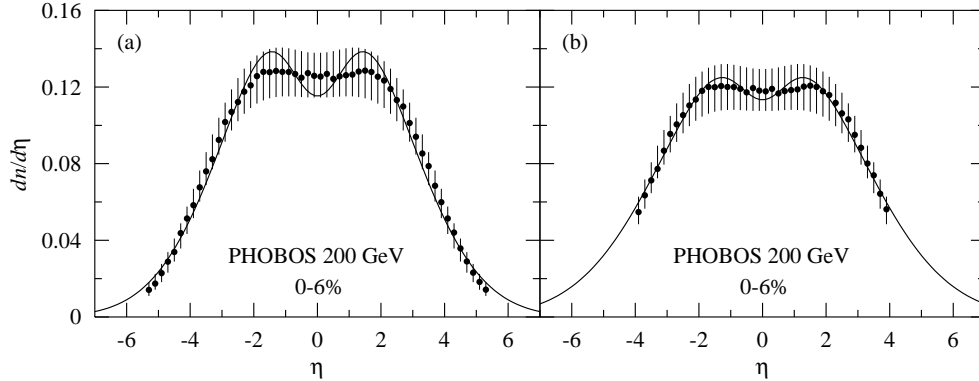


Fig. 4. Analyses of $dn/d\eta$ by means of single Gaussian and Eq. (7). (a) Data in full- η variable are described by $V^2(t) = 5.27 \pm 0.26$ and $m/p_t = 1.13 \pm 0.10$. The best $\chi^2 = 20.0/51$. (b) Data in $|\eta| < 4.0$ are used, i.e., $4.0 < |\eta| < 5.4$ are neglected. $V^2(t) = 7.41 \pm 0.85$ and $m/p_t = 0.82 \pm 0.13$ are used. The best $\chi^2 = 4.0/37$. Introduction of renormalization is necessary, due to the Jacobian

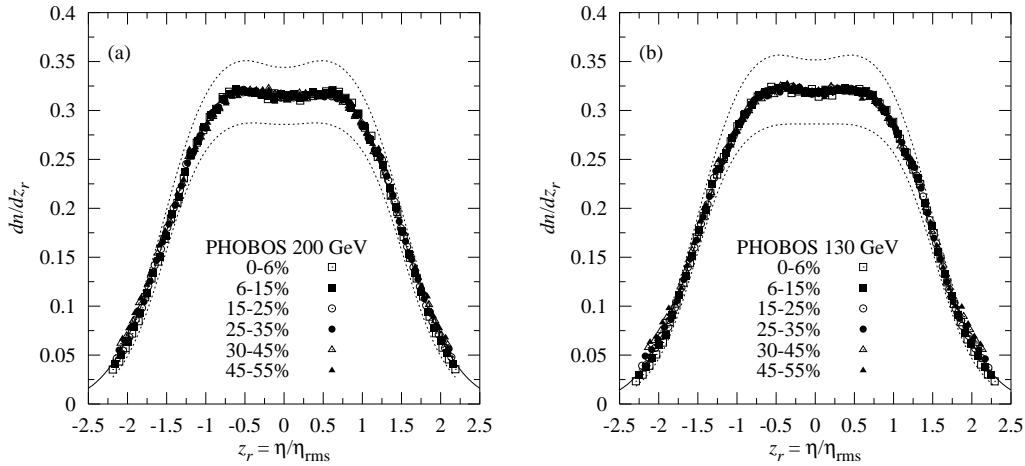


Fig. 5. Normalized distribution of dn/dz_r with $z_r = \eta/\eta_{rms}$ scaling and estimated parameters using Eq. (3). (a) $\sqrt{s_{NN}} = 200$ GeV, $p = 0.867 \pm 0.002$, $V_r^2(t) = 0.506 \pm 0.011$, $\chi^2/n.d.f. = 14.6/321$. (b) $\sqrt{s_{NN}} = 130$ GeV, $p = 0.854 \pm 0.002$, $V_r^2(t) = 0.494 \pm 0.010$, $\chi^2/n.d.f. = 25.5/321$. Dashed lines are magnitudes of error-bars. Notice that $\langle z_r^2 \rangle = z_{max}(1 - p) + V_r^2 \neq 1.0$, due to the sum of two Gaussian distributions.

of $[\text{sec}^{-1} = (1/3) \times 10^{-23} \text{ fm}^{-1}]$. The magnitude of the interaction region in Au-Au collision is assumed to be 10 fm. See, for example, Ref. 7). t is estimated as

$$t \approx 10 \text{ fm}/c \approx 3.3 \times 10^{-23} \text{ sec.} \quad (8)$$

The frictional coefficient and the variance are obtained in Table III. They are comparable with values $[\tau_Y^{-1} = 0.1 - 0.08 \text{ fm}^{-1}]$ of Ref. 8), which have been obtained from the proton spectra at SPS collider.

5. *Concluding remarks* c1) We have analyzed $dn/d\eta$ distribution by Eqs. (2)

Table III. Values of γ and σ^2 at $\sqrt{s_{NN}} = 200$ GeV provided that $t \approx 3.3 \times 10^{-23}$ sec.

centrality (%)	45-55	35-45	25-35	15-25	6-15	0-6	average
γ [fm ⁻¹]	0.096	0.099	0.100	0.101	0.103	0.104	0.101
σ^2 [fm ⁻¹]	0.817	0.800	0.763	0.720	0.696	0.666	0.744
σ^2/γ	8.51	8.08	7.63	7.13	6.76	6.40	7.42

and (6). The intercepts c 's do not show remarkable energy dependence*).

c2) We have shown that the dip structures in $dn/d\eta$ are hardly explained only by the Jacobian factor from dn/dy in Fig. 4. What the authors of Refs. 5) and 6) have stressed is the explanation on the dip structures of $dn/d\eta$ in the central region ($|\eta| < 4.0$) by the Jacobian factor. This situation should be changed in analyses of $dn/d\eta$ in the whole pseudo-rapidity region. (See Fig. 4.)

c3) From the evolution parameter t with γ using the assumption for the size of interaction ($R(\text{Au} + \text{Au}) \approx 10$ fm), we have estimated the frictional coefficient which is almost consistent with values at SPS energies in Ref. 8)

c4) From dn/dz_r 's at $\sqrt{s_{NN}} = 200$ GeV and 130 GeV, we have shown that both distributions are coincided with each other. If there are no labels (200 GeV and 130 GeV) in Fig. 5, we cannot distinguish them. This coincidence means that there is no particular change in $dn/d\eta$ between $\sqrt{s_{NN}} = 200$ GeV and 130 GeV.

Acknowledgements The authors would like to thank Dr. R. Nouicer for his kind communication concerning the data. Various conversations with A. Bialas, H. Boggild, J. P. Bondorf, T. Csorgo, T. Hirano, R. Hwa, H. Ito, S. Muroya, K. Tuominen and G. Wolschin are very useful for the present study. One of authors (M.B.) would like to acknowledge The Scandinavia-Japan Sasakawa Foundation for financial support to his stay at Niels Bohr Institute.

-
- 1) M. Biyajima, M. Ide, T. Mizoguchi and N. Suzuki, Prog. Theor. Phys. **108** (2002) 559 and Addenda (to appear). See also hep-ph/0110305.
 - 2) B. B. Back et al. [PHOBOS Collaboration], Phys. Rev. Lett. **87** (2001), 102303.
 - 3) R. Nouicer et al., [PHOBOS Collaboration], nucl-ex/0208003.
 - 4) M. M. Aggarwal *et al.* [WA98 Collaboration], Eur. Phys. J. C **18** (2001) 651.
 - 5) D. Kharzeev and E. Levin, Phys. Lett. B **523** (2001), 79.
 - 6) K. J. Eskola, K. Kajantie, P. V. Ruuskanen and K. Tuominen, Phys. Lett. B **543** (2002), 208.
 - 7) K. Morita, S. Muroya, C. Nonaka and T. Hirano, nucl-th/0205040; to appear in Phys. Rev. C.

*) We have observed that the intercepts c are decreasing as the colliding energy increases: c (130 GeV) = 0.125–0.138 \rightarrow c (200 GeV) = 0.123–0.130. From the semi-phenomenological analyses, i.e., Eq. (6), the reason is attributed to the changed ratio $A^{(200 \text{ GeV})}/A^{(130 \text{ GeV})} = 1.15$ and decreased ratio $N_{\text{ch}}(130 \text{ GeV})/N_{\text{ch}}(200 \text{ GeV}) \approx 0.82$. $1.15 \times 0.82 \approx 0.94$. On the other hand, in the view of the stochastic approach, i.e., Eq. (2), the reason is mainly attributed to the $\eta_{\text{max}} = \ln(\sqrt{s_{NN}}/m_N)$ as

$$\frac{c(200 \text{ GeV})}{c(130 \text{ GeV})} = \frac{V(t)^{(200)}}{V(t)^{(130)}} \exp \left[-\frac{\eta_{\text{max}}^{2(200)}}{2V^2(t)^{(200)}} + \frac{\eta_{\text{max}}^{2(130)}}{2V^2(t)^{(130)}} \right] \approx 0.94,$$

where the suffixes mean colliding energies.

- 8) G. Wolschin, Eur. Phys. J. A **5** (1999), 85.